



HAL
open science

A multidating approach applied to historical slackwater flood deposits of the Gardon River, SE France

L. Dezileau, B. Terrier, J.F. Berger, P. Blanchemanche, A. Latapie, R. Freydier, L. Bremond, André Paquier, M. Lang, J.L. Delgado

► **To cite this version:**

L. Dezileau, B. Terrier, J.F. Berger, P. Blanchemanche, A. Latapie, et al.. A multidating approach applied to historical slackwater flood deposits of the Gardon River, SE France. *Geomorphology*, 2014, 214, p. 56 - p. 68. 10.1016/j.geomorph.2014.03.017 . hal-01059669

HAL Id: hal-01059669

<https://hal.science/hal-01059669>

Submitted on 1 Sep 2014

HAL is a multi-disciplinary open access archive for the deposit and dissemination of scientific research documents, whether they are published or not. The documents may come from teaching and research institutions in France or abroad, or from public or private research centers.

L'archive ouverte pluridisciplinaire **HAL**, est destinée au dépôt et à la diffusion de documents scientifiques de niveau recherche, publiés ou non, émanant des établissements d'enseignement et de recherche français ou étrangers, des laboratoires publics ou privés.

A multidating approach applied to historical slackwater flood deposits of the Gardon River, SE France

L.Dezileau^{a,*}, B.Terrier^b, J. F.Berger^c, P.Blanchemanche^d, A.Latapie^e,
R.Freydier^f, L.Bremond^g, A.Paquier^e, M.Lang^e, J.L.Delgado^h

^aGeosciences Montpellier, Université Montpellier 2, CNRS, UMR 5243, France

^bAgence de l'eau Rhône-Méditerranée et Corse, Lyon cedex, France

^cEnvironnement Ville et Société, Université Lumière Lyon 2, CNRS, France

^dArchéologie des Sociétés Méditerranéennes, CNRS, UMR 5140, France

^eIrstea, UR HHLY, CS 70077, Villeurbanne, France

^fHydrosciences Montpellier, Université Montpellier 2, CNRS, UMR 5569, France

^gCentre de Bio-Archéologie et d'Ecologie, EPHE, Université Montpellier 2, CNRS, UMR 5059, France

^hCETE Méditerranée, Aix-en-Provence, France

* Corresponding author: UMR 5243 CC60 UM2/CNRS, Place E. Bataillon 34095 Montpellier cedex 5, France. Fax:
+33 (0) 4 67 14 49 30 ;E-mail: laurent.dezileau@gm.univ-montp2.fr.

Geomorphology, 214, 56-68, <http://dx.doi.org/10.1016/j.geomorph.2014.03.017>

25 **Abstract**

26 A multidating approach was carried out on slackwater flood deposits, preserved in valley side
27 rock cave and terrace, of the Gardon River in Languedoc, southeast France. Lead-210, caesium-
28 137, and geochemical analysis of mining-contaminated slackwater flood sediments have been
29 used to reconstruct the history of these flood deposits. These age controls were combined with
30 the continuous record of Gardon flow since 1890, and the combined records were then used to
31 assign ages to slackwater deposits. The stratigraphic records of terrace GE and cave GG were
32 excellent examples to illustrate the effects of erosion/preservation in a context of a progressively
33 self-censoring, vertically accreting sequence. The sedimentary flood record of the terrace GE
34 located at 10 m above the channel bed is complete for years post-1958 but incomplete before.
35 During the 78-year period 1880-1958, 25 floods of a sufficient magnitude ($> 1450 \text{ m}^3/\text{s}$) have
36 covered the terrace. Since 1958, however, the frequency of inundation of the deposits has been
37 lower: only 5 or 6 floods in 52 years have been large enough to exceed the necessary threshold
38 discharge ($> 1700 \text{ m}^3/\text{s}$). The progressive increase of threshold discharge and the reduced
39 frequency of inundation at the terrace could allow stabilisation of the vegetation cover and
40 improved protection against erosion from subsequent large magnitude flood events. The
41 sedimentary flood record seems complete for cave GG located at 15 m above the channel bed.
42 Here, the low frequency of events would have enabled a high degree of stabilisation of the
43 sedimentary flood record, rendering the deposits less susceptible to erosion.

44 Radiocarbon dating are used in this study and compared to the other dating techniques. Eighty
45 percent of radiocarbon dates on charcoals were considerably older than those obtained by the
46 other techniques in the terrace. On the other hand, radiocarbon dating on seeds provided better
47 results. This discrepancy between radiocarbon dates on charcoal and seeds is explained by the

48 nature of the dated material (permanent wood vs. annual production and resistance to degradation
49 process). Finally, we showed in this study that although the most common dating technique used
50 in paleoflood hydrology is radiocarbon dating, usually on charcoal preserved within slackwater
51 flood sediments, this method did not permitus to define a coherent age model. Only the combined
52 use of lead-210, caesium-137, and geochemical analysis of mining-contaminated sediments with
53 the instrumental flood record can be applied to discriminate and date the recent slackwater
54 deposits of the terrace GE and cave GG.

55
56 *Keywords:* paleoflood hydrology; floods; hydraulic modelling; lead-210; caesium-137; radiocarbon
57 dating; historical record of mining activity

58 **1. Introduction**

59 Palaeoflood hydrology is the reconstruction of the magnitude and frequency of large floods using
60 geological evidence (Baker et al., 2002). Methods and concepts of paleohydrology have been
61 described extensively in the literature (e.g., Kochel et al., 1982; Ely and Baker, 1985; Baker,
62 1987; Benito and Thorndycraft, 2005). Only some of the general concepts are briefly reiterated
63 here. The methodology combines (i) stratigraphic and sedimentologic analyses to identify the
64 number of flood units preserved within a particular sedimentary sequence; (ii) hydraulic
65 modelling to calculate minimum discharge estimates from the known elevations of slackwater
66 flood sediments; (iii) dating techniques to determine the chronology of flood occurrence; and (iv)
67 establishment of possible links between past climatic changes and the frequency/magnitude of
68 flood events. Although the main aim of palaeoflood hydrology is to lengthen the flood series
69 beyond that of the instrumental record, significant benefits can also be gained by accurately
70 dating modern slackwater flood deposits (Thorndycraft et al., 2004a,b). As these events occurred

71 during the instrumental period, the potential to correlate the modern sedimentary flood record
72 with the data measured at gauging stations is possible. This is of particular importance in
73 understanding the palaeoflood record preserved over centennial timescales (Benito et al., 2004).

74
75 In this study, ^{14}C , ^{210}Pb , and ^{137}Cs dating and geochemical analyses (Pb and Al concentrations)
76 were carried out on slackwater flood deposits, preserved in valley side rock cave and terrace, of
77 the Gardon River in Languedoc in southeast France (Fig. 1). The study sites are located near
78 Remoulins where a gauging station has been operational over the last 130 years. This provided
79 the potential for correlation between the instrumental and sedimentary flood records. The two
80 largest floods of the twentieth and twenty-first centuries, namely the 1958 and 2002 events (with
81 estimated discharges of $6400\text{ m}^3/\text{s}$ and $7200\text{ m}^3/\text{s}$, respectively, at Remoulins, compared to a
82 mean annual flow of $33\text{ m}^3/\text{s}$) occurred during the dating range of the ^{137}Cs and ^{210}Pb methods,
83 thereby providing the potential for comparison between these events and palaeofloods. Finally,
84 our analysis of slackwater flood deposits illustrates important uncertainties related to stratigraphic
85 studies of paleofloods. These uncertainties bear directly on related limitations in individual event
86 discrimination and temporal resolution of typical slackwater paleoflood records caused by effects
87 of erosion/preservation in a context of a progressively self-censoring vertically accreting
88 sequence.

89

90 **2. Dating techniques**

91 Different techniques are available to date recent slackwater deposits. ^{137}Cs dating has been used
92 for determining the chronology of modern sediment deposits. ^{137}Cs is an artificial radionuclide
93 that was first released into the atmosphere by nuclear bomb testing in the mid-1950s. The

94 temporal patterns of ^{137}Cs input are characterized by a first peak in 1959 and a second peak at
95 1962-1964; the termination of ^{137}Cs input occurred around mid-1980s. Some areas may have had
96 an additional input in 1986 after the Chernobyl incident. ^{137}Cs reached the land surface by
97 atmospheric fallout. The accumulation of ^{137}Cs in sedimentary deposits throughout the world
98 therefore began by the early to mid-1950s (e.g., Popp et al., 1988). Analysis of ^{137}Cs has been
99 applied to fine-grained deposits to quantify soil erosion and lake sedimentation rates (e.g., Ritchie
100 et al., 1974; Sutherland, 1989), to date oxbow sedimentation and modern fine-grained floodplain
101 sediments (Popp et al., 1988; Walling and He, 1997; Bonté et al., 2001; Stokes and Walling,
102 2003). However, ^{137}Cs is strongly adsorbed to clay particles and is transported with the
103 suspended load rather than in solution (McHenry and Ritchie, 1977). The detectable activity of
104 ^{137}Cs is related to the clay content of the sediments (McHenry and Ritchie, 1977; Popp et al.,
105 1988), which poses a potential problem when the technique is applied to alluvial deposits with
106 relatively low clay content. Studies analysing the post-bomb ^{137}Cs content in modern slackwater
107 flood deposits from the San Francisco, Paria rivers in Arizona and from the Llobregat River in
108 Spain (Ely et al., 1992; Thorndycraft et al., 2005b) have shown that the technique can also be
109 successfully applied to date fluvial sediments characterized by a mix of fine and coarser particles.
110 The ^{137}Cs dating results from the Gardon River study reaches can be tested using the combined
111 data of palaeoflood stratigraphy, discharge estimation by hydraulic modelling and the
112 instrumental discharge record.

113
114 The basic methodology of ^{210}Pb dating was established in a seminal paper by Golberg (1963).
115 ^{210}Pb precipitates from the atmosphere through ^{222}Rn decay and accumulates in surface soils,
116 glaciers, or lakes where successive layers of material are buried by later deposits. ^{210}Pb
117 deposition on land is primarily owing to meteoric fallout; and it is adsorbed quickly and

118 tenaciously by the surfaces of fine sediments, primarily onto clays, where, even more so than
119 ^{137}Cs , it is chemically immobile (Cremers et al., 1988). There it undergoes beta decay to ^{210}Bi
120 with a half-life of 22.3 years. ^{210}Pb fallout is generally found to be constant at any given location
121 over time scales relevant to ^{210}Pb geochronology (Appleby and Oldfield, 1978, 1992; He and
122 Walling, 1996). In the simplest model, the initial $(^{210}\text{Pb})_{\text{ex}}$ is assumed constant and thus $(^{210}\text{Pb})_{\text{ex}}$ at
123 any time is given by the radioactive decay law. The sedimentation rates in slackwater flood
124 deposits are clearly variable and discontinuous because of the near-instantaneous sedimentation
125 of flood deposits so that this type of model is difficult to use (He and Walling, 1996; Aalto and
126 Nittrouer, 2012). However, this technique can be successfully applied to assess whether an
127 apparent accumulation of 'fresh sediment' exists (<100 years, i.e., ~4 to 5 times its decay period of
128 22.3 years). ^{210}Pb dating will be tested in the Gardon River.

129
130 Carbon-14 analysis is the standard technique for dating Holocene alluvial deposits. Radiocarbon
131 dating of slackwater flood sediments has an applicable age range of between ca. 300 and 55,000
132 yBP (Trumbore, 2000) and therefore cannot accurately date the sediments of flood events from
133 the most recent centuries. With atmospheric testing of nuclear weapons after 1950, ^{14}C activity in
134 the troposphere rapidly increased, reaching a peak of 100% above normal in the early 1960s
135 (Nydal and Lovseth, 1983). For post-bomb alluvial deposits, radiocarbon dating on organic
136 materials preserved within slackwater flood sediments gives a 'modern age' that can be useful to
137 assess whether an apparent accumulation of "fresh sediment" exists in the study area. The ^{14}C age
138 of organic materials entrained in an alluvial deposit may differ significantly from the actual age
139 of the deposit, depending on the residence time of the organics within the environment (Ely et al.,
140 1992). Thus, for flood deposits, the type of organic material available constrains the accuracy of
141 the resulting dates. In particular, detrital wood and charcoal can predate fluvial deposits by

142 several hundred years (Atwater et al., 1990). The radiocarbon dating is not the best technique to
143 accurately date the sediments of flood events from the most recent centuries (Trumbore, 2000)
144 but was used in this study to be tested by obtaining radiocarbon dates for several types of plant
145 materials from well-dated flood deposits.

146

147 Ages for modern flood deposits can be correctly assigned with the use of trace metals generated
148 by mining activity. This geochemical analysis of mining-contaminated floodplain sediments has
149 been used to date floodplain sediment and slackwater flood deposits where a known historical
150 record of mining within the catchment exists (e.g., Davies and Lewin, 1974; Lewin et al., 1977;
151 Hindel et al., 1996; Knox and Daniels, 2002; Thorndycraft et al., 2004a,b). The extraction of Zn–
152 Pb from the Gardon River basin started in 1730 (Elbaz-Poulichet et al., 2006). The number of
153 mining concessions increased significantly between 1860 and 1930. During this period, mining
154 activity generated 400,000 tons of tailings. Between 1951 and 1963, Pennaroya and then
155 Metaleurop mining companies extensively exploited the ore generating between 2,300,000 and
156 5,000,000 tons of tailings (30,000 tons of lead and 3500 tons of Zn). This mining activity ceased
157 in 1993. One of the most important mines on the Gardon River basin is the Carnoules mine,
158 which has generated a total of 1,500,000 tons of wastes. The mine officially closed on 24
159 October 1963. In September 1976, the tailings partially collapsed caused by a violent
160 Mediterranean thunderstorm. This was followed in October 1976 by the sudden evacuation of the
161 100,000 m³ of water initially contained in a lake that had formed in the tailing stock. The accident
162 was responsible for a major pollution of water and soil in the Gardon River basin (DREAL,
163 2008). This paper describes a combined stratigraphic and geochemical approach to identify traces
164 of historic tin mining activity within slackwater deposits of the Gardon River.

165

166 **3. Gardon River basin flood hydrology**

167 *3.1. Study area description*

168 The Gardon River watershed (1858 km² at Remoulins) is located in the southeast Massif Central
169 mountains and is ~ 135 km long from its headwaters at 1699 m above sea level (Mount Lozere)
170 to its confluence with the Rhône River at 6 m asl (Fig. 1A). The Gardon is the southern most
171 tributary of the Rhône River. In terms of geology (Fig. 1B), the Cévennes Mountains are mainly
172 composed of Paleozoic granite, schist, gneiss, and sandstone (Bonnifait et al., 2009). The rivers
173 present a high degree of sinuosity in this upstream area. Farther downstream, the Gardon River
174 crosses the Gard plains, which are based on Mesozoic carbonate formations with a stratigraphical
175 series ranging from Jurassic (west) to Cretaceous (east). Close to the Cévennes Mountains, this
176 secondary series is interrupted by a network of NE–SW faults that delineate the Alès graben, a
177 1500-m graben filled with Tertiary sediments from the Oligocene period. The river then crosses
178 Cretaceous limestone following deep canyons (the Gardon gorges). These limestone formations
179 present a high degree of karstification. Downstream, the Mesozoic formations are covered with
180 the Quaternary sediments of the Rhône River (Bonnifait et al., 2009). The high watershed of the
181 Gardon River was reforested during the nineteenth century by calcic or acidophile medio-european
182 beech species, white oak species, *Castanea sativa* forests, and shrublands with *Juniperus*
183 *communis*. The limestone tableland of Nîmes garrigue, mainly occupied by forests of green oaks
184 (*Quercus ilex* and *Quercus rotundifolia*), some white oak coppice, a mosaic of a substeppic
185 grassland with annual grasses from the *Thero-brachypodietea*. The Matorral tree with
186 *Juniperus phoenicea* occupies the rocky ledges of the limestone tableland, while on the rocky
187 slopes develop xero-thermophilic formations with *Buxus sempervirens*. The limestone
188 canyon includes riparian vegetation composed mainly of *Salix alba*, *Populus alba*, and *Fraxinus*

189 *excelsior*, with some pines (*Aleppo* and *Pinion pines*) on pediments and upper alluvial terraces.

190

191 *Insert Fig. 1 near here*

192

193 The study sites are located in the middle reach of the Gardon River in the Cretaceous bedrock
194 gorge, between Russan and Remoulins. Little to no changes in the shape of the canyon occurred
195 throughout the late Holocene. The identification of flood sediment sources transported into the
196 gorge is facilitated by the strong contrast between the granitic, basaltic, and metamorphic bedrock
197 of the upper catchment and the carbonates of the Gardon gorge. Slackwater flood sediments have
198 been deposited and preserved on high-standing terraces along channel margins and in many
199 karstic caves and alcoves.

200

201

202 *3.2. Flood hydrology and hydroclimatology*

203 The Gardon River has a typically Mediterranean regime with a low mean annual discharge (33
204 m³/s, SAGE des Gardons, 2000), extreme seasonal variations, and flood peaks around 100 times
205 greater than the mean discharge. Mean annual rainfall in the catchment varies from 500 to 1100
206 mm. Nuissier et al. (2008) provided a detailed analysis of typical flash flood events in this region.
207 Large amounts of precipitation can accumulate over several days, particularly at the end of
208 summer and beginning of autumn, as frontal disturbances slow down and are reinforced by the
209 relief of the Massif Central. When a Mesoscale Convective System remains quasistationary for
210 several hours, heavy rainfall of over 200 mm can be recorded in less than a day and can therefore
211 lead to devastating flash floods.

212 A large set of hydrological data is available from the flood forecasting service (known as the
213 ‘Service de Prevision des Crues’ or SPC30) and the local authority (‘Smage des Gardons’). The
214 gauging station located at Remoulins (~15 km downstream of study sites) provides stage
215 observations from 1890 onward (Fig.2). Since 1890, three major flood events have been recorded
216 with water levels > 7 m and estimated peak flood discharges defined from the stage-discharge
217 relationship > 5000 m³/s, namely the 16-17 October 1907 (5300 m³/s), 4 October 1958 (6400
218 m³/s), and 8-9 September 2002 (7000 m³/s) floods. This last extreme flood event claimed the
219 lives of 23 people and caused €1.2 billion worth of damage to towns and villages along the river.
220 Seven thousand houses were damaged, 100 of which were completely destroyed and 1500
221 submerged under 2 m of water (Huet et al., 2003).

222

223
224

Insert Fig. 2 near here

225 *3.3. Previous paleoflood studies of the Gardon River*

226 One paleoflood study of the Gardon River has been conducted just downstream of our study area
227 (Sheffer et al., 2008). The main objectives of their study were (i) to provide an accurate and
228 reliable discharge estimation of the 2002 flood at the study reach, (ii) to reconstruct a record of
229 major flood events using paleoflood hydrology, and (iii) to improve the understanding of the
230 2002flood magnitude and consider the long-term perspective of rare events and extreme flood
231 discharges provided by the paleoflood record. They concluded that according to slackwater
232 deposits found at different sites at least five extreme events occurred during the Little Ice Age.
233 Each was larger than the 2002 flood (Sheffer et al., 2008).

234

235

236 **4. Methods**

237 *4.1. Paleoflood analysis*

238
239 During large floods in canyons, slackwater deposits(usually fine sands and silts) accumulate
240 relatively rapidly from suspension in sites of abrupt drop in flow velocity (Ely and Baker, 1985;
241 Kochel and Baker, 1988; Benito et al., 2003a). As a result, a layer of these deposits is formed.
242 This sediment may be preserved in protected sites, such as caves and alcoves in the canyon walls,
243 and backwater zones behind valley constrictions (Kochel et al., 1982; Ely and Baker, 1985; Baker
244 and Kochel, 1988; Enzel et al., 1994; Springer, 2002; Webb and Jarrett, 2002; Benito et al.,
245 2003b; Benito and Thorndycraft, 2005). Subsequent flood deposits may accumulate above this
246 layer by floods with stages higher than the top of the depositional sequence (Baker, 1987).

247
248 For this study, two depositional sequences (Fig. 3) were investigated along the Gardon River in a
249 high-standing, terrace-like bench of aggrading sediments (GE located at 10 m above the channel
250 bed, the base of the terrace is at 2 m, the terrace is 70 m wide and 300 m long) and in a cave (GG
251 at 15 m above the channel bed). Sites of slackwater flood sediment deposition were identified
252 along the study reaches, and sections were cut to expose the sedimentary sequences. Individual
253 flood units were determined through a close inspection of depositional breaks and/or indicators of
254 surficial exposure (e.g., presence of a paleosol, clay layers at the top of a unit, detection of
255 erosional surfaces, bioturbation features, angular clast layers deposits in local alcoves or slope
256 material accumulation between flood events, fireplaces, and anthropogenic occupation layers
257 between flood events).

258 *Insert Fig. 3 near here*

259

260 4.2. Analytical methods
261

262 Dating of sedimentary layers was carried out using ^{210}Pb and ^{137}Cs methods on a centennial
263 timescale. Both nuclides together with U, Th, and ^{226}Ra were determined by gamma spectrometry
264 at the Géosciences Montpellier Laboratory. The 1-cm-thick sediment layers were sieved in order
265 to obtain the fraction smaller than 1 mm. This material was then finely crushed after drying and
266 transferred into small gas-tight PETP (polyethylene terephthalate) tubes (internal height and
267 diameter of 38 and 14 mm, respectively), and stored for more than 3 weeks to ensure equilibrium
268 between ^{226}Ra and ^{222}Rn . The activities of the nuclides of interest were determined using a
269 Canberra Ge well detector and compared with the known activities of an in-house standard.
270 Activities of ^{210}Pb were determined by integrating the area of the 46.5-keV photo-peak. ^{226}Ra
271 activities were determined from the average of values derived from the 186.2-keV peak of ^{226}Ra
272 and the peaks of its progeny in secular equilibrium with ^{214}Pb (295 and 352 keV) and ^{214}Bi (609
273 keV). In each sample, the (^{210}Pb unsupported) excess activities were calculated by subtracting the
274 (^{226}Ra supported) activity from the total (^{210}Pb) activity. Note that, throughout this paper,
275 parentheses () denote activities. Activities of ^{137}Cs were determined by integrating the area of the
276 661-keV photo-peak. Error bars on ($^{210}\text{Pbex}$) and (^{137}Cs) do not exceed 6%.

277 The ^{14}C analyses were conducted at the Laboratoire de Mesure ^{14}C (LMC14) on the ARTEMIS
278 accelerator mass spectrometer in the CEA Institute at Saclay (Atomic Energy Commission).
279 These ^{14}C analyses were carried out with the standard procedures described by Tisnérat-Laborde
280 et al. (2001). The ^{14}C ages were converted to calendar years using the CALIB 6.1.0 calibration
281 program (Stuiver and Reimer, 1993). A summary of the samples submitted for dating, and their
282 associated results, is presented in Table 1. All radiocarbon dates are quoted in the text as the 2σ
283 calibrated age range.

284

285

Insert Table 1 near here

286

287

288 Before analysis, sediment samples were ground in an agate mortar and digested in a Teflon beaker
289 on a hot plate. One hundred milligrams of sediment were digested using a three step procedure:
290 1/H₂O₂, 2/HF:HNO₃:HClO₄, and 3/HNO₃:HCl. The Al and Pb concentrations were determined
291 using an ICP-MS, X Series II (Thermo Fisher Scientific), equipped with a CCT (Collision Cell
292 Technology) chamber at the Hydrosiences Montpellier Laboratory. Certified reference material
293 from LGC Standards, i.e., LGC6189 (river sediment), was used to check analytical accuracy and
294 precision. Measured concentrations agree with recommended values to within 10% (Al) and 3%
295 (Pb). To find out if there was an enrichment of lead relative to the local baseline, an enrichment
296 factor (EF) technique was used. The enrichment factor (EF) of lead is calculated following the
297 equation: $EF_{Pb} = (Pb/Al)_{sample} / (Pb/Al)_{Average\ Local\ Background}$.

298 The $(Pb/Fe)_{sample}$ is the ratio of Pb and Fe concentration of the sample and $(Pb/Fe)_{Average\ Local}$
299 $background$ is the ratio of Pb and Fe concentration of a background. The background concentrations
300 of Pb were taken from the base of the terrace (i.e., pre-industrial period concentrations).
301 Grainsize analysis was conducted on contiguous 1 cm samples using a Beckman-Coulter
302 LS13320 laser diffraction particlesize analyser at the Géosciences Montpellier Laboratory. Grain
303 size distribution measurements were made on the < 1 mm sediment fraction.

304

305 *4.3. Hydraulic modelling*

306 *4.3.1. Model description*

307 A one-dimensional (1D) hydraulic model of the Gorges was built using RubarBE, a numerical
308 model that solves the shallow water equations and uses an explicit second-order Godunov-type
309 scheme (El kadi Abderrezzak and Paquier, 2009). The modelled reach is ~31.5 km long and
310 extends from Russan, located at the entrance of the Gorges, to downstream of the Remoulins
311 gauging station, located at the exit of the Gorges. Topographic data were obtained from the
312 SPC30 and the Smage des Gardons. In addition, two surveying campaigns were carried out in the
313 Gorges in order to obtain detailed topographic data near the paleoflood sites. During these
314 campaigns, 21 profiles were surveyed with a Leica TC 305 total station and a differential GPS
315 Leica 1200 with GPS-GLONASS receptor. In total, 95 profiles were used to construct the
316 hydraulic model. The 2002 flood hydrographs provided by the SPC30 at Russan and Remoulins
317 gauging stations revealed that the peak flows were approximately the same at both locations. In
318 order to simulate past flood events, it was therefore decided that the flow at Remoulins be used as
319 an upstream boundary condition at Russan. The downstream boundary condition has been
320 defined with the water levels available at the Remoulins gauging station.

321 A sensitivity analysis has been conducted to assess the influence of the Alzon River, a tributary
322 draining an area of 203 km², on the water levels calculated at the paleoflood sites.

323

324 *4.3.2. Model calibration*

325 Following the 2002 flood event, a post-event analysis of debris lines and observed water levels
326 was conducted by the Smage des Gardons. The model was thus calibrated on the 21 water levels
327 available for the 2002 event and validated on the 10 water levels recorded for the 1958 event. On
328 average, the difference between the measured water levels and the results of the model is -0.11 m
329 with a standard deviation of 0.69 m for the 2002 flood event. For the 1958 event, the average
330 difference is -0.95 m with a standard deviation of 0.94 m. Most of the debris lines surveyed are

331 located in the vicinity of hydraulic singularities such as bridges. The flow behaviour in these
332 areas is notably difficult to reproduce in a 1D hydraulic model. Furthermore, the levels of the
333 debris lines in the vicinity of the bridge may not be representative of the highest mean water level
334 and may be the result of water surface fluctuations that cannot be reproduced by the 1D model.
335 The results of the calibration are therefore regarded as satisfactory.

336

337 *Insert Fig. 4 near here*

338

339 *4.3.2. Sensitivity analysis*

340 The results of the model with the varying roughness coefficient allow the determination of an
341 envelope of stage discharge relationship at the two paleoflood sites (Fig. 4B). The sensitivity
342 analysis on the flow record used as an upstream boundary condition in the model also provides an
343 envelope on the water levels and discharges at the paleosites for each flood event. Results are
344 then compared with the historical flood records available at Remoulins to identify the events that
345 may have reached or submerged the sites (Fig.4C). Envelopes at the paleoflood sites are bound
346 by the scenarios of the sensitivity analysis of $Q \pm 10\%$ combined with the scenarios of $K_s \pm 10\%$.
347 These results can be put into perspective with the dating approach and are discussed in the
348 following paragraphs.

349

350 **5. Results**

351 *5.1. Stratigraphic records of flood events in terrace GE and cave GG*

352 *5.1.1. Terrace GE*

353 At terrace GE, the stratigraphy consists of 20 individual slackwater flood units. Based on the

354 results of the hydraulic model (stage-discharge curve), a flood event of intensity similar to that of
355 the 1972 event ($\sim 2100 \text{ m}^3/\text{s}$ at Remoulins) is required for a flood event to cover the uppermost
356 flood unit of the terrace. Figure 5 presents $^{210}\text{Pb}_{\text{ex}}$ and ^{137}Cs activities and the enrichment factor
357 of Pb for this terrace. Also illustrated is the minimum discharge estimate calculated for the
358 floodwaters to cover the terrace during flood events.

359 The ^{137}Cs activity is recorded in flood units GE17, GE18, GE19, and GE20, with maximum
360 values of 38 and 45 mBq/g in units GE17 and GE18, respectively (Fig.5). No ^{137}Cs is found in
361 the older deposits of the profile. The first post-1955 event, identified by the first trace of ^{137}Cs
362 activity in the profile, is that of GE17 indicating that the four flood deposits GE17-GE20 all post-
363 date this period. More particularly, the high ^{137}Cs activity recorded in flood units GE17 and
364 GE18 (38 and 45 mBq/g) can be associated to the maximum atmospheric production in the mid-
365 1960s (around 1963, Fig. 5).

366 The first flood unit containing $^{210}\text{Pb}_{\text{ex}}$ activity is unit GE15 located at 90 cm depth in the
367 stratigraphic profile, with a value of 5 mBq/g. The $^{210}\text{Pb}_{\text{ex}}$ activity is recorded in flood units GE15,
368 GE17, GE18, GE19, and GE20, with a maximum value of 58 mBq/g in unit GE19. There is an
369 apparent accumulation of 'fresh sediment' (< 100 years, i.e., approximately 4 to 5 times the
370 decay period of ^{210}Pb) in the uppermost part of the terrace GE. The $^{210}\text{Pb}_{\text{ex}}$ can help us to confirm
371 a number of results produced using ^{137}Cs dating technique. The high $^{210}\text{Pb}_{\text{ex}}$ activity recorded in
372 flood units GE19 and its exponential decrease in the other flood deposits (GE18 to G15) suggests
373 that the uppermost part of the terrace can be considered as being stratifically undisturbed. In
374 particular, the first trace of $^{210}\text{Pb}_{\text{ex}}$ activity in the profile is that of GE15, thereby indicating that
375 the six flood deposits GE15-GE20 are recent and all post-date approximately the end-1910s (Fig.
376 7).

377 The geochemistry of the profile shows that enrichment factor (EF) of Pb, with a range of 1.0 to
378 10.5, exhibits very high variation between the base and the top of the terrace (Fig. 5). The lowest
379 EF values of Pb (around 1.0) occur in flood units between GE1 and GE9. The EF is higher in the
380 uppermost flood units of the terrace, around 1.9 between GE10 and GE17, 3.3 in GE18, 10.5 in
381 GE19, while it decreases in the last flood unit GE20 (3). At 155 cm depth, an increase in the EF
382 of Pb occurs from a background value of 1.0 (GE9) to a value of 1.9 (GE11). The increase
383 production of Pb between 1870 and 1905 could explain these increased levels of heavy metals
384 (Fig 5). In terms of the relative chronology, therefore, the geochemical analysis shows that the
385 lower stratigraphic slackwater deposits units (GE1 to GE9) are probably older than 1870. The EF
386 of Pb is higher in the uppermost flood units of the terrace, around 3.3 in GE18 and 10.5 in GE19.
387 The first high EF of 3.3 can be linked to the strong increase of Pb production during the mid-
388 1960s (GE18) and the very high EF of 10.5 to the major pollution of the basin in 1976 (GE19,
389 Fig. 5).

390
391 In addition to the trace metal, ^{137}Cs and $^{210}\text{Pb}_{\text{ex}}$ activities as age marker horizons, extreme floods
392 during the last 50 years also produced very prominent stratigraphic horizon. These age controls
393 were combined with the continuous record of stage available from 1890 at the Remoulins
394 gauging station located 15 km downstream (data from SPC 30). The combined records were then
395 used to assign ages to slackwater deposits indicative of other large floods in the GE sequence
396 (Fig 5). The 1958 event, the second largest in instrumental record ($6400 \text{ m}^3/\text{s}$), deposited a 25-
397 cm- thick unit of medium sands (GE16: $270 \mu\text{m}$). The next three flood units (GE17, GE18, and
398 GE19) are well marked by the pollution of Pb and ^{137}Cs and have been assigned to three lower
399 magnitude floods (4000 , 2900 , and $3000 \text{ m}^3/\text{s}$, respectively) that occurred in 1963, 1969, and

400 1976, respectively (Fig. 5). Thin sedimentary layers and fine sands characterize these three flood
401 units. The 2002 event, the largest in the instrumental record, deposited a 30-cm- thick unit of
402 medium sands (GE20). From these different flood units, a positive correlation ($r^2=0.96$) exists
403 between the magnitude of the flood versus the grain size/thickness of the different units. The
404 sedimentary flood record prior to 1958 at site GE seems incomplete, as indicated by the fact that
405 fewer post-pollution flood units are preserved (seven units since 1890) than there were flood
406 events with a discharge of sufficient magnitude to cover the sedimentary surface (Fig. 5). Based
407 on the results of the hydraulic model, about 25 flood events would have submerged terrace GE
408 between 1870 ($>1430 \text{ m}^3/\text{s}$) and 1958 ($>1700 \text{ m}^3/\text{s}$) for the scenario for a roughness coefficients
409 K increased by 10% and input flows overestimated by 10% (Figs. 4C and 5). Assuming that a
410 minimum depth of water is required above the site in order for the sediment to deposit in a
411 sufficiently thick layer, it is possible that events of lower magnitudes are not recorded in the
412 sedimentary record. In that case, based on the possible relationship between sediment grain size
413 and magnitude, GE15 could be associated to 1951, GE14 to 1943, GE13 to 1933, GE12 to 1915,
414 GE11 to 1907, GE10 to 1900, and GE9 to 1890 (Fig. 5). Erosion, errors in hydrological
415 documentary sources, and model approximation could also be at the origin of this low correlation
416 between sedimentary flood record and the continuous record of Gardon flow between 1890 and
417 1958.

418

419 *Insert Fig. 5 near here*

420

421 5.1.2. Cave GG

422 Cave GG is located at 15 m above the channel bed with a minimum estimated discharge of
423 approximately $4500 \text{ m}^3/\text{s}$ required for floodwaters to reach the site (Fig. 4c). Results from the

424 hydraulic model suggest that at least three events have submerged GG. Cave GG contains more
425 than 1.5 m of slackwater flood sediments. In this article, only the upper 35 cm will be discussed.
426 Six depositional units were found on the first 35 cm, four of which correspond to flood deposits
427 (Fig.6). The flood deposits consist of fine sand to silt, featuring diffused lamination, with many
428 charcoal pieces and ash lens. Median grain size (d50) is clearly affected by the presence of
429 charcoals and ash lens. The ^{137}Cs data indicates activity in only one sample analysed in the upper
430 part of the profile (GG4 with a value of 2 mBq/g). The same pattern is observed for $^{210}\text{Pb}_{\text{ex}}$
431 activity (Fig. 6). ^{210}Pb activity is recorded in the flood unit GG4 (14mBq/g), with no activity in
432 the older deposits. The presence of ^{137}Cs activity and $^{210}\text{Pb}_{\text{ex}}$ activity in this unit means that the
433 age of GG4 post-date 1955 (Fig. 6). At 15 cm depth, a slight increase in the EF of lead occurs
434 (from a background value of 1 to a value of 1.4). The increase production of lead between 1870
435 and 1905 could explain this increased level of heavy metals occurring in the slackwater deposit
436 GG2 (Fig 6). The EF of lead is higher in the uppermost flood units of the terrace, around 2.2 in
437 GG3 and 4.4 in GG4. The high EF of 2.2 and more in this unit means that the age of GG3 and
438 GG4 post-date the beginning of the twentieth century but cannot be associated to precise
439 ages. The combined records were then used to assign ages to slackwater deposits indicative of
440 other large floods in the GG sequence (Fig. 6). The 1907 event, the third largest in instrumental
441 record (5200 m³/s), deposited a 5-cm- thick unit of fine sands (GG2). The next flood unit,
442 assigned to the second largest in instrumental record (1958:6300 m³/s), deposited a 5-cm- thick
443 unit of fine sands (GG3). The 2002 event, that is the largest in the instrumental record, deposited
444 a 4-cm- thick unit of fine sands (GG4). The 1961 and 1976 events did not reach the cave and may
445 explain why the EF of Pb is not higher than 4.4.

446

447

Insert Fig. 6 near here

448
449 *5.2. Radiocarbon dating*
450 In the fluvial terrace GE, 17 dates were obtained using conventional radiocarbon analysis on
451 wood charcoals and seeds. All of the obtained dates are plotted in Fig. 7 in yBP (corrected for
452 isotopic fractionation) and calibrated to calendar years. From this recent terrace GE, one would
453 normally expect progressively younger dates in the uppermost flood units of the terrace. For
454 radiocarbon analysis on charcoals, at the exception of the first two radiocarbon dates in GE1 (200
455 yBP) and GE2 (285 yBP), radiocarbon dates are older than expected for the basal part of the
456 terrace GE but considerably older (between 520 and 6540 yBP) than those obtained by the other
457 techniques in the uppermost flood units of the terrace. Uncalibrated ^{14}C ages of seeds are often in
458 an inverted stratigraphic position. However, when these ages are calibrated at 2σ they are
459 consistent with those obtained by the other dating techniques.

460

461 *Insert Fig. 7 near here*

462

463

464 **6. Discussion**

465

466 *6.1. Dating techniques*

467

468 Ages for modern flood deposits have been correctly assigned with the use of ^{137}Cs . The presence
469 or absence of ^{137}Cs in these flood deposits of the Gardon River is not controlled by the particle
470 size distribution. In the upper four deposits (units 17 through 20), ^{137}Cs was detected even in the

471 sample with the lowest clay content ($F < 2\mu\text{m}: 0.03\%$) (Fig. 5). Moreover, the uppermost pre-bomb
472 deposit (unit 15) showed no ^{137}Cs activity. There was no leaching of ^{137}Cs into the post-bomb
473 deposits from the overlying post-bomb deposits, as no samples below unit 16 showed detectable
474 ^{137}Cs . Four samples from the flood deposit G20 (2002) showed ^{137}Cs activity, although
475 atmospheric ^{137}Cs fallout is negligible during this period. The presence of ^{137}Cs in this recent
476 flood deposit could have resulted from the erosion and redeposition of post-1950 floodplain or
477 terrace deposits. Our results are consistent with other authors (Ely et al., 1992; Thorndycraft et
478 al., 2005a,b), who found that (i) ^{137}Cs is concentrated by erosion and redeposition of fine-grained
479 sediments and (ii) significant ^{137}Cs activity in sandy sediments indicates that high clay content is
480 not necessary for this method to be effective in distinguishing pre- and post-1950 deposits.

481 The $^{210}\text{Pb}_{\text{ex}}$ confirms a number of results produced using the ^{137}Cs dating technique. The high
482 $^{210}\text{Pb}_{\text{ex}}$ activity recorded in flood units GE19 and its exponential decrease in the other flood
483 deposits (GE18 to G15) suggests that the uppermost part of the terrace is recent (< 100 years,
484 i.e., ~ 4 to 5 times its decay period of 22.3 years) and can be considered as being stratigraphically
485 undisturbed. Significant $^{210}\text{Pb}_{\text{ex}}$ activity in sandy sediments indicates that high clay content is also
486 not necessary for this method to be used. However, without clay-normalized absorbed $^{210}\text{Pb}_{\text{ex}}$
487 activity and without using a model of ^{210}Pb input during floods, this approach is not sufficiently
488 accurate for dating episodic sediment accumulation on terraces (Aalto and Nittrouer, 2013).

489 Ages for modern flood deposits have been correctly assigned with the use of lead generated by
490 mining activity. The latest sediment deposit GE20 (2002) presents EF of lead similar to those of
491 1969. This latest sedimentary deposit (GE20) might reflect remobilization of ancient floodplain
492 sediments, acting as a secondary contamination source during large flood events. However, the
493 similarity of EF values in the 2002 flood deposit and in current stream sediments (E. Resongles,

494 HSM, personal communication, 2014), rather points out limited improvement of sediment quality
495 by waste water treatment over recent years. Interestingly, the values of EF of Pb in units GG3 and
496 GG4 (1958 and 2002 events in cave GG) are the same that in the equivalent flood event in the
497 sequence GE16 and GE20 (1958 and 2002 events in terrace GE). This would suggest that each
498 flood event is characterized by an EF of Pb. This result also means that the EF ratio of Pb is not
499 controlled by the particle size distribution. If this is confirmed in later studies, EF of Pb could be
500 used as another proxy for dating flood deposits in this study area.

501 Eighty percent of dates on charcoal samples are much older than is reasonably expected (Fig. 7).
502 In the GE terrace, the prevailing inversion of dates, with many of these recording ages older than
503 expected, is most likely a response to remobilization of sediment. The Gardon River does not
504 transport material downslope in direct fashion from upstream source areas to our study site
505 during a single, rapid flood event, but rather in a process that comprises several episodic floods,
506 small channel migration events on the Gard plain between the Alès graben and Gardon gorges is
507 envisioned. During extreme flood events, the inundated area is considerably increased and may
508 cover a part of the old terraces. Sediment is temporarily stored until it is exposed by small
509 channel migration or erosion of old terraces, mobilized and then once again redeposited. Other
510 processes may affect the radiocarbon dating techniques on charcoals such as alteration of
511 samples, by percolation, infiltration from underlying sections (Evans, 1985; Tornqvist et al.,
512 1998), or hardwater effect (a term for the old-carbon reservoir derived from dissolved carbonate
513 rocks; Saarnisto, 1988). Sediments of large flood deposits in GE and GG contain a high
514 proportion of quartz, (>45%), illite/mica (>45%), and relatively little carbonate or dolomite
515 (<3%). These minerals present in flood deposits derive mainly from the erosion of Paleozoic
516 granite, schist, and gneiss rocks in the upper part of the Gardon drainage basin. Charcoals have
517 probably the same origin, i.e., coming from the combustion of trees that initially lived in the

518 Cévennes Mountains. Thus, consistent with the origin of the sediment, our radiocarbon dates do
519 not have a significant hardwater error, i.e., not initially affected by an oldcarbon reservoir.
520 Another possible explanation lies in the industrial past of the study area. The Gardon watershed
521 presents numerous coal mines, which were extensively exploited during the nineteenth and
522 twentieth centuries. The sediment of terrace GE contains a high proportion of small graphite
523 particles (~ 80% of the carbon material in the different flood units sieved). Therefore, it can also
524 be suggested that the binding of small particles of dead carbon on the charcoal produce an aging
525 of the ^{14}C ages. We estimated the induced aging process by adding 10% of a dead carbon on a
526 charcoal dated to 1950. Ten percent is a relatively high value. In this case, this charcoal would
527 have an age of 1079 years AD ($1950 - t_{\text{modern } ^{14}\text{C with 10\% of dead carbon}} = 1950 - \ln(100/90) * 8266.6$),
528 which cannot explain the results of the radiocarbon dating on charcoals. To conclude, all these
529 other processes alone may not account for the extremely wide range in age offset and chronologic
530 error; and the remobilization of sediment is probably the first process, which can affect our
531 radiocarbon dates.

532 Radiocarbon dating on seeds seems to give better results. Almost two reasons may explain this
533 dating difference between charcoal and seeds. Firstly, the seed is an annual product of a living
534 plant when charcoal is produced by incomplete combustion of a living or dead tree/shrub,
535 possibly very old. This effect is called 'inbuilt age' or 'old wood effect' (Gavin, 2001) because
536 woody plants maintain old tissues in their structure; branches and stems could be greatly older
537 than the date of the fire event and even more than the flood event. Thus the ^{14}C date of a charcoal
538 might be significantly older than a ^{14}C date of a seed in the same flood unit. Secondly, charcoals
539 are relatively large and decay-resistant, they are likely to remain in the vicinity of the riverbank a
540 longer time than smaller and more readily decomposed seeds (Oswald et al., 2005). At site GE,
541 the seeds probably have a local origin. The identified seeds are essentially *Polycnemonum*, *Carex*,

542 *Sambucus ebulus*, and *Medicago*, which grow presently on the riverbank. However, although
543 dating of seeds provides better results than charcoal, the accuracy of this technique is limited
544 because of the large uncertainty of the ^{14}C dates compared to discrete flood events. Only the
545 combined use of ^{210}Pb , ^{137}Cs and geochemical analysis of mining-contaminated sediments with
546 the instrumental flood record can be applied to discriminate and date the recent slackwater
547 deposits of the terrace GE and cave GG.

548

549 *6.2. Uncertainties affecting record completeness*

550 The principal goal of a typical slackwater paleoflood investigation is to enumerate floods
551 represented in the stratigraphic record as accurately and completely as possible and to determine
552 their timing as precisely as possible (Kochel and Baker, 1988). This task is influenced by several
553 types of uncertainty, which include the effects of stratigraphic ambiguity, erosion, internal
554 stratigraphic complexity, incomplete exposure, pedogenesis, stratigraphic record self-censoring
555 (House et al., 2002), and the uncertainties for dating slackwater flood sediments. Taking into
556 account these effects have important implications for evaluating the information content of
557 regional or site-specific fluvial paleoflood data. The stratigraphic records of GE and GG are
558 excellent examples to illustrate the effects of erosion/preservation in a context of a progressively
559 self-censoring vertically accreting sequence. The sedimentary flood record between 1958 and
560 2010 at site GE seems complete. Prior to 1958, this record is incomplete, as indicated by the fact
561 that fewer post-pollution flood units (seven units) are preserved than there were flood events with
562 a discharge of sufficient magnitude to cover the sedimentary surface (25 events approximately).
563 As suggested, the most likely cause of this incomplete record is erosion. The second largest flood
564 on record was that of 1958; however, the stratigraphy suggests that this event was not responsible
565 for the erosion of earlier deposits. The contact between units GE15 and GE16 is characterized by

566 buried soils, and no evidence of an erosive contact is observed. It is likely, therefore, that the
567 sedimentary record reflects a change in preservation potential of the sediments as distinct from
568 the erosive capability of a particular flood. During the 78-year period 1880-1958, 25 floods of a
569 sufficient magnitude ($> 1450 \text{ m}^3/\text{s}$) have covered the terrace. Since 1958, however, the frequency
570 of inundation of the deposits has been lower, there have only been five or six floods in 52 years
571 large enough to exceed the necessary threshold discharge ($> 1700 \text{ m}^3/\text{s}$). The progressive increase
572 of threshold discharge and the reduced frequency of inundation at the terrace could allow
573 stabilisation of the vegetation cover and improved protection against erosion from subsequent
574 large magnitude flood events (the extreme 2002 event has not eroded the buried soils of the 1976
575 event). A high frequency of events would not have enabled such a high degree of stabilisation,
576 rendering the deposits more susceptible to erosion. In cave GG located 15 m above the channel
577 bed, the sedimentary flood record between 1907 and 2010 seems complete, as indicated by the
578 fact that there are as many post-pollution flood units (three units) preserved as flood events with a
579 discharge of sufficient magnitude to cover the sedimentary surface (three events: 1907, 1958, and
580 2002). Here, the low frequency of events would have enabled a high degree of stabilisation of the
581 sedimentary flood record, rendering the deposits less susceptible to erosion. This higher
582 stabilisation is also probably facilitated by a strong decrease of the flood current velocity in this
583 cave. To conclude, at low elevation sites, frequent flooding may erode the slackwater flood
584 sediments (e.g., the lower part of terrace GE). In contrast, deposits in high elevation caves or
585 terraces (largest floods) may have a larger preservation potential, since only extreme events are
586 able to flush away the sediments accumulated at these higher sites. These observations are not
587 new. They have been stated previously in the paleoflood literature with varying degrees of
588 emphasis (House et al., 2002; Thorndycraft et al., 2005a,b). However, our study in the Gardon
589 River illuminated several types of uncertainties and suggested several others with an excellent

590 example to illustrate the effects of erosion/preservation in a context of a progressively self-
591 censoring, vertically accreting sequence.

592

593 *6.3. Relation to other paleoflood records in the region*

594

595 Sheffer et al. (2008) described a series of 10 distinct slackwater deposits in a cave 12 m above the
596 river bed (cave GH) at 400 m downstream of the GE site. From this cave, Sheffer et al. (2008)
597 deduced an increase of flood events during the Little Ice Age and to a cold and wet phase around
598 2850 years ago. This is an important result because it allowed us to highlight a link between flood
599 events and climate variability at the regional and southern European scale. Cave GH is located at
600 an elevation below the 2002 flood water level representing low magnitude floods, and slackwater
601 deposits matched a minimum associated discharge of 2600 m³/s. Cave GH contains at least
602 seven units deposited in the last 2000 years (Sheffer et al., 2008). Assuming a minimum discharge
603 of 2600 m³/s, the upper part of this cave should record at least eight flood events during the
604 twentieth century and not only seven during the last 2000 years. This discrepancy could be related
605 to erosion because of the low position of the cave or to erroneous radiocarbon dates. As observed
606 in terrace GE where 80% of dates on charcoal samples are much older than is reasonably
607 expected, radiocarbon ages on charcoal samples of slackwater deposits in cave GH could also be
608 erroneous in the uppermost part of this cave. To conclude, a supplementary geochronological
609 study of this alluvial sequence would be necessary to confirm or not these first
610 palaeohydrological results of Sheffer et al. (2008).

611

612

613

614 **8. Conclusion**

615 Our detailed paleoflood investigation on the Gardon River has shown some strengths and
616 weaknesses of slackwater paleoflood hydrology as a technique for improving understanding of
617 the frequency of floods in bedrock channels. ^{210}Pb , ^{137}Cs , and geochemical analysis of mining-
618 contaminated sediments have been used to reconstruct the history of slackwater flood deposits.
619 This approach was combined with the continuous record of Gardon water levels since 1890 to
620 assign ages to slackwater deposits. At cave GG and fluvial terrace GE, respectively located at 15
621 and 10 m above the channel bed, these dating techniques have been successfully applied and
622 illustrate the potential of this multidating approach in dating recent slackwater flood deposits.
623 The sedimentary flood record was complete in cave GG but not in terrace GE. We deduced that
624 at low elevation sites, frequent flooding could erode the slackwater flood sediments (e.g., the
625 lower part of terrace GE). In contrast, deposits in high elevation caves or terraces (largest floods)
626 could have a larger preservation potential, as only extreme events were able to flush away the
627 sediments accumulated at these higher sites.

628 Most ^{14}C dates on wood charcoal samples (80%) in the terrace GE were much older than the age
629 reasonably expected. In the terrace, the prevailing inversion of dates, with so many of these
630 recording ages older than expected, was most likely a clear response to fluvial remobilization of
631 sediment and their organic contents. Radiocarbon dating on seeds seems to give better results and
632 could be explained by an absence of 'inbuilt age' effect and low decay-resistance compared to
633 wood charcoals. However, although the dating of seeds provides better results than wood
634 charcoal, the accuracy of this technique is limited to date flood events from the most recent
635 centuries. Only the combined use of ^{210}Pb , ^{137}Cs , and geochemical analysis of mining-

636 contaminated sediments with the instrumental flood record can be applied to discriminate and
637 date the recent slackwater deposits of the terrace GE and cave GG.

638

639 **Acknowledgements**

640

641 This project was totally funded by the ANR commission (EXTRAFLO project). The authors wish
642 to thank Thierry Montecinos, Marie Bouchet, Stéphanie Garnero, Isabelle Avril, Cyril Soustelle,
643 Neri for their help in fieldwork; the IRSTEA team for doing bathymetric cross sections; the DDE
644 Nîmes for the historical flood data; Laurent Bouby for seeds identifications. We thank the
645 Laboratoire de Mesure ^{14}C (LMC14) ARTEMIS in the CEA Institute at Saclay (French Atomic
646 Energy Commission) for the ^{14}C analyses (EXTRAFLO project). We thank the three anonymous
647 reviewers for their constructive comments on the manuscript.

648

649 **References**

650

- 651 Aalto, R., Nitttrouer, C., 2012. ^{210}Pb geochronology of flood events in large tropical river
652 systems. (2012). *Phil. Trans. R. Soc. A* 370, 2040–2074.
- 653 Appleby, P. G., Oldfield, F., 1978. The calculation of Pb-210 dates assuming a constant rate of
654 supply of unsupported Pb-210 to the sediment. *Catena* 5, 1–8.
- 655 Appleby, P., Oldfield, F., 1992. Application of lead-210 to sedimentation studies. In: Ivanovich,
656 M., Harmon, R.S., (Eds.), *Uranium Series Disequilibrium, Application to Earth, Marine and*
657 *Environmental Sciences*. Clarendon Press, Oxford, UK, pp. 773–778.
- 658 Atwater, B.F., Trumm, D.A., Tinsley, J.D., III, Stein, R.S., Tucker, A.B., Donahue, D.J., Jull,
659 A.J.T., Payen, L.A. 1990. Alluvial plains and earthquake recurrence at the Coalinga
660 anticline. In Rymer, M.J., Ellsworth, W.L. (Eds.), *The Coalinga, California, Earthquake of*
661 *May 2, 1983*. Publisher City, ST, pp. 273-297, 1487.
- 662 Baker, V.R., 1987. Paleoflood hydrology and extraordinary flood events. *Journal of Hydrology*

- 663 96, 79–99.
- 664 Baker, V.R., Kochel, R.C., 1988. Flood sedimentation in bedrock fluvial systems. In: Baker,
665 V.R., Kochel, R.C., Patton, P.C. (Eds.), *Flood Geomorphology*. Wiley, city,USA, pp. 123–
666 137.
- 667 Baker, V.R., Webb, R.H., House, P.K., 2002. The scientific and societal value of paleoflood
668 hydrology. In: House, P.K., Webb, R.H., Baker, V.R., Levish, D.R. (Eds.), *Ancient Floods,
669 Modern Hazards: Principles and Applications of Paleoflood Hydrology*. Water Science and
670 Application Series, vol. 5, AGU, Washington, DC, pp. 127– 146.
- 671 Benito, G., Sopena, A., Sanchez, Y., Machado, M.J., Perez Gonzalez, A., 2003a. Palaeoflood
672 record of the Tagus River (central Spain) during the late Pleistocene and Holocene.
673 *Quaternary Science Reviews* 22, 1737–1756.
- 674 Benito, G., Sanchez-Moya, Y., Sopena, A., 2003b. Sedimentology of high-stage flood deposits of
675 the Tagus River, central Spain. *Sedimentary Geology* 157, 107–132.
- 676 Benito, G., Lang, M., Barriendos, M., Llasat, M.C., Frances, F., Ouarda, T., Thorndycraft, V.R.,
677 Enzel, Y., Bardossy, A., Coeur, D., Bobee, B., 2004. Use of systematic, palaeoflood and
678 historical data for the improvement of flood risk estimation. Review of scientific methods.
679 *Nat. Hazards* 31, 623–643.
- 680 Benito, G., Thorndycraft, V.R., 2005. Palaeoflood hydrology and its role in applied hydrological
681 sciences. *Journal of Hydrology* 313, 3–15.
- 682 Bonnifait, L., Delrieu, G., Le Lay, M., Boudevillain, B., Masson, A., Belleudy, P., Gaume E.,
683 Saulnier, G.-M., 2009. Hydrologic and hydraulic distributed modelling with radar rainfall
684 input: reconstruction of the 8-9 September 2002 catastrophic flood event in the Gard region,
685 France. *Advances in Water Resources* 32, 1077–1089.
- 686 Bonté, P., Ballais, J.L., Masson, M., Ben Kehia, H., Eyraud, C., Garry, G., Ghram, A., 2001.
687 Datations au ^{137}Cs , ^{134}Cs et ^{210}Pb de dépôts de crues du XXe siècle. *Datation, XXIe
688 rencontres internationales d'archéologie et d'histoire d'Antibes*, Ed. APDCA, 141–157.
- 689 Cremers, A., Elsen, A., De Preter, P., Maes, A. 1988. Quantitative analysis of radiocaesium
690 retention in soils. *Nature* 335, 247–249.
- 691 Davies, B.E., Lewin, J., 1974. Chronosequences in alluvial soils with special reference to historic
692 lead pollution in Cardiganshire, Wales. *Environ Pollut* 6, 49–57.
- 693 DREAL, 2008. Internet site: <http://basol.developpement-durable.gouv.fr/>

- 694 El kadi Abderrezzak, K., Paquier, A., 2009. One-dimensional numerical modeling of sediment
695 transport and bed deformation in open channels. *Water Resour. Res.* 45, W05404.
- 696 Elbaz-Poulichet, F., Bruneel, O., Casiot, C., 2006. The Carnoules mine. Generation of As-rich
697 acid mine drainage, natural attenuation processes and solutions for passive in-situ
698 remediation. *Documentation IRD*, p 1–8.
- 699 Ely, L.L., Baker, V.R., 1985. Reconstructing paleoflood hydrology with slackwater deposits
700 Verde River, Arizona. *Physical Geography* 6, 103–126.
- 701 Ely, L.L., Webb, R.H., Enzel, Y., 1992. Accuracy of post-bomb ^{137}Cs and ^{14}C in dating fluvial
702 deposits. *Quaternary Research* 38, 196–204.
- 703 Enzel, Y., Ely, L.L., Martinez, J., Vivian, R.G., 1994. Paleofloods comparable in magnitude to
704 the catastrophic 1989 dam failure flood on the Virgin River, Utah and Arizona. *Journal of*
705 *Hydrology* 153, 291–317.
- 706 Evans, L.J., 1985. Dating methods of Pleistocene deposits and their problems. VII. Paleosols.
707 In:ed. Rutter, N.W. (Ed.), *Dating Methods of Pleistocene Deposits and Their Problems*. Repr.
708 Ser. Geosci. Canada, Toronto, Canada, pp. 53–59.
- 709 Gavin, D.G., 2001. Estimation of inbuilt age in radiocarbon ages of soil charcoal for fire history
710 studies. *Radiocarbon* 43, 27–44.
- 711 Golberg E., 1963. Geochronology with ^{210}Pb . *Radioactive Dating*. International Atomic
712 Energy Agency, Vienna, Austria, pp. 121–31.
- 713 He, Q., Walling, D.E., 1996. Interpreting particle size effects in the adsorption of ^{137}Cs and
714 unsupported ^{210}Pb by mineral soils and sediments. *J. Environ. Radioact* 30, 117–137.
- 715 Hindel, R., Schlich, J., De Vos, W., Ebbing, J., Swennen, R., Van Keer, Y., 1996. Vertical
716 distribution of elements in overbank sediment profiles from Belgium, Germany and The
717 Netherlands. *Journal of Geochemical Exploration* 56, 105–122.
- 718 House, P.K., Pearthree, P.A., Klawon, J. E., 2002. Historical Flood and Paleoflood Chronology
719 of the Lower Verde River, Arizona: Stratigraphic Evidence and Related Uncertainties. In :
720 House, P. K., Webb, R. H., Baker, V. R., Levish D. R., (Eds.), *Ancient Floods, Modern*
721 *Hazards*, American Geophysical Union, Washington, D.C., pp. 267–293.
- 722 Huet, P.X., Martin, J.L., Prime, P., Foin, C., Laurain, P., Cannard, 2003. Retour d'expérience
723 décrues de septembre 2002 dans les départements du Gard, de l'Hérault, du Vaucluse, des
724 Bouches du Rhône, de l'Ardeche et de la Drome. *Rapport de l'Inspection Générale de*

- 725 l'Environnement. Ministre de l'Ecologie et du Développement Durable, République
726 Française. 133 pp. Available at the Internet site:
727 <http://www.environnement.gouv.fr/infoprat/Publications/publi-ige.htm>.
- 728 Knox, J.C., Daniels, J.M., 2002. Watershed scale and the stratigraphic record of large floods. In :
729 House, P. K., Webb, R. H., Baker, V. R., Levish, D. R., (Eds.), *Ancient Floods, Modern
730 Hazards*, American Geophysical Union, Washington, D.C., pp. 237–255.
- 731 Kochel, R.C., Baker, V.R., Patton, P.C., 1982. Palaeohydrology of southwest Texas. *Water
732 Resour. Res.* 18, 1165–1183.
- 733 Kochel, R.C., Baker, V.R., 1988. Paleoflood analysis using slack water deposits. In: Baker, V.R.,
734 Kochel, R.C., Patton, P.C. (Eds.), *Flood Geomorphology*. John Wiley and Sons, U.S.A., pp.
735 357–376.
- 736 Lewin, J., Davies, B.E., Wolfenden, P.J., 1977. Interaction between channel change and historic
737 mining sediments. In K.J. Gregory (Ed.), *River channel changes*, pp. 353–367.
- 738 McHenry, J.R., Ritchie, J.C., 1977. Physical and chemical parameters affecting transport of
739 ^{137}Cs in arid watersheds. *Water Resources Research* 13, 923–927.
- 740 Nuissier, O., Ducrocq, V., Ricard, D., Lebeauvin, C., Anquetin, S., 2008. A numerical study of
741 three catastrophic precipitating events over southern France. I: Numerical framework and
742 synoptic ingredients. *Quart. J. Roy. Meteor. Soc.* 134, 111–130.
- 743 Nydal, R., Lovseth, K., 1983. Tracing bomb ^{14}C in the atmosphere 1962–1980. *Journal of
744 Geophysical Research* 88, 3621–3642.
- 745 Oswald, W.W., Anderson, P.M., Brown, T.A., Brubaker, L.B., Hu, F.S., Lozhkin, A.V., Tinner,
746 W., Kaltenrieder, P., 2005. Effects of sample mass and macrofossil type on radiocarbon
747 dating of arctic and boreal lake sediments. *The Holocene* 15, 758–767.
- 748 Popp, C. J., Hawley, J. W., Love, D. W., Dehn, M., 1988. Use of radiometric (^{137}Cs , ^{210}Pb),
749 geomorphic, and stratigraphic techniques to date recent oxbow sediments in the Rio Puerto
750 Drainage. Grants Uranium Region, New Mexico. *Environmental Geology and Water Science*
751 3, 253–269.
- 752 Ritchie, J.C., McHenry, J.R., Gil, A.C., 1974. Fallout ^{137}Cs in the soils of three small
753 watersheds. *Ecology* 55, 887–890.
- 754 Saarnisto, M., 1988. Time-scales and dating. In: Huntley, B., Webb III, T. (Eds.), *Vegetation
755 History*. Handbook of vegetation science. Kluwer Academic Publishers, Dordrecht, pp. 77–

- 756 112.
- 757 SAGE des Gardons, 2000. Annexe 1 au Schéma d'Aménagement et de Gestion des Eaux des
758 gardons, SAGE, pp 187.
- 759 Sheffer, N.A., Rico, M., Enzel, Y., Benito, G., Grodek, T., 2008. The palaeoflood record of the
760 Gardon River, France: A comparison with the extreme 2002 flood event. *Geomorphology* 98,
761 71–83.
- 762 Springer, G.S., 2002. Caves and their potential use in paleoflood studies. In: House, P.K., Webb,
763 R.H., Baker, V.R., Levish, D.R. (Eds.), *Ancient Floods, Modern Hazards: Principles and*
764 *Applications of Paleoflood Hydrology*. Water Science and Applications, AGU, pp. 329–344.
- 765 Stokes, S., Walling, D.E., 2003. Radiogenic and isotopic methods for the direct dating of fluvial
766 sediments. In: Kondolf, M., Piegay, H. (Eds.), *Tools in Fluvial Geomorphology*. Wiley,
767 Chichester, pp. 233–267.
- 768 Stuiver, M., Reimer, P.J.. 1993. Extended 14C data base and revised CALIB 3.0 14C age
769 calibration program. *Radiocarbon* 35, 1, 215–30.
- 770 Sutherland, R.A., 1989. Quantification of accelerated soil erosion using the environmental tracer
771 Caesium-137. *Land Degradation and Rehabilitation* 1, 199–208.
- 772 Thorndycraft, V.R., Benito, G., Rico, M., Sopena, A., Sánchez-Moya, Y., Casas-Planes, A.,
773 2004a. A Late Holocene Paleoflood record from slackwater flood deposits of the Llobregat
774 River, NE Spain. *Journal Geological Society of India* 64 (4), 549–559.
- 775 Thorndycraft, V., Brown, A.G. , Pirrie, D., 2004b. Alluvial records of Medieval and prehistoric
776 tin mining on Dartmoor, SW England. *Geoarchaeology*, 19, 219–236.
- 777 Thorndycraft, V., Benito, G., Rico, M., Sopena, A., Sánchez-Moya, Y., Casas, A., 2005a.
778 Paleoflood hydrology of the Llobregat River, NE Spain: a 3000year record of extreme
779 floods. *Journal of Hydrology* 313 (1-2), 16–31.
- 780 Thorndycraft, V.R., Benito, G., Walling, D.E., Sopena, A., Sanchez-Moya, Y., Rico, M., Casas,
781 A., 2005b. Caesium-137 dating applied to slackwater flood deposits of the Llobregat River,
782 N.E. Spain. *Catena* 59, 305–318.
- 783 Tisnérat-Laborde, N., Poupeau, J.J., Tannau, J.F., Paterne, M., 2001. Development of a
784 semiautomated system for routine preparation of carbonate samples. *Radiocarbon* 43, 299–
785 304.
- 786 Tornqvist, T.E., Van Ree, M.H.M., Van't Veer R., Van Geel B., 1998. Improving methodology

787 for high-resolution reconstruction of sealevel rise and neo-tectonics and paleoecological
788 analysis and AMS 14C dating of basal peats. *Quat. Res.* 49, 72–85
789 Trumbore, S.E., 2000. Radiocarbon geochronology. In: Noller, J.S., Sowers, J.M., Lettis, W.R.
790 (Eds.), *Quaternary Geochronology: Methods and Applications*. AGU, Washington, D.C., pp.
791 41–60.
792 Walling, D.E., He, Q., 1997. Use of fallout 137Cs in investigations of overbank sediment
793 deposition on river floodplains. *Catena* 29, 263–282.
794 Webb, R.H., Jarrett, R.D., 2002. One-dimensional estimation techniques for discharges of
795 paleofloods and historical floods. In: House, P.K., Weeb, R.H., Baker, V.R., Levish, D.R.
796 (Eds.), *Ancient Floods, Modern Hazards: Principles and Applications of Paleoflood*
797 *Hydrology*. Water Resources Monograph, vol. 5. AGU, Washington, D.C., pp. 111–12.

798

799

800

801

802

803 **List of figures and table**

804

805 Fig. 1: Topography, hydography, and geological maps of the Gardon river watershed.

806

807 Fig. 2: Annual maximum gage height available at Remoulins between 1890 and 2010.

808

809 Fig. 3: (A) A map showing the study sites in the Gardon Gorges. (B) Terrace (GE) and cave
810 (GG), sites of slackwater flood sediment archives .

811

812 Fig. 4 (A) Cross sections of the paleosites used in the model; (B) Calculated stage-discharge
813 relationships and their envelope and (C) Historical flood series at Remoulins.

814

815 Fig. 5. The proposed chronology for the terrace GE slackwater flood deposits, d_{50} , ^{137}Cs
816 activities, $^{210}\text{Pb}_{\text{ex}}$ activities, EF of lead, the peak annual instantaneous discharges series at
817 Remoulins. The envelope on the range of discharges at Remoulins that may have submerged the
818 site resulting from the sensitivity analysis is shown. The individual slackwater flood units
819 deposited by a particular event are annotated.

820

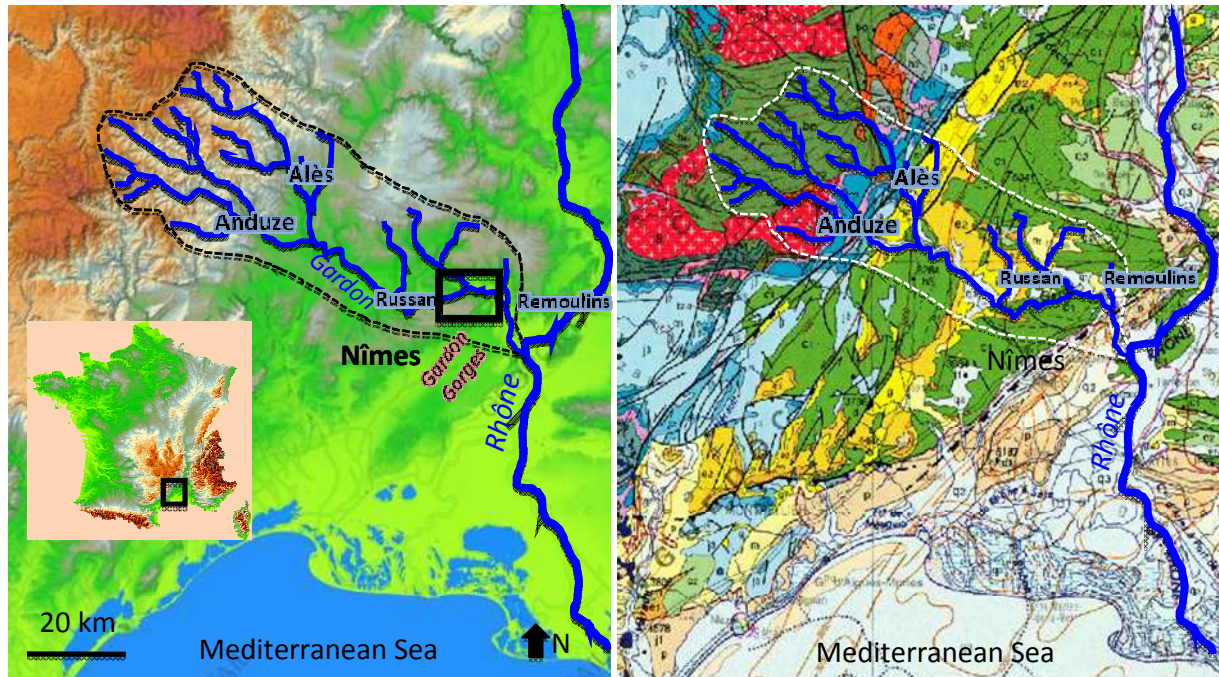
821 Fig. 6. The proposed chronology for the cave GG slackwater flood deposits, d_{50} , ^{137}Cs activities,
822 $^{210}\text{Pb}_{\text{ex}}$ activities, the peak annual instantaneous discharges series at Remoulins. The envelope on
823 the range of discharges at Remoulins that may have submerged the site resulting from the
824 sensitivity analysis is shown. The individual slackwater flood units deposited by a particular
825 event are annotated.

826

827 Fig. 7. Stratigraphy and age model of site GE. Radiocarbon ages on wood charcoals (in blue) and
828 seeds (in red) in BP and calendar ages (2σ)

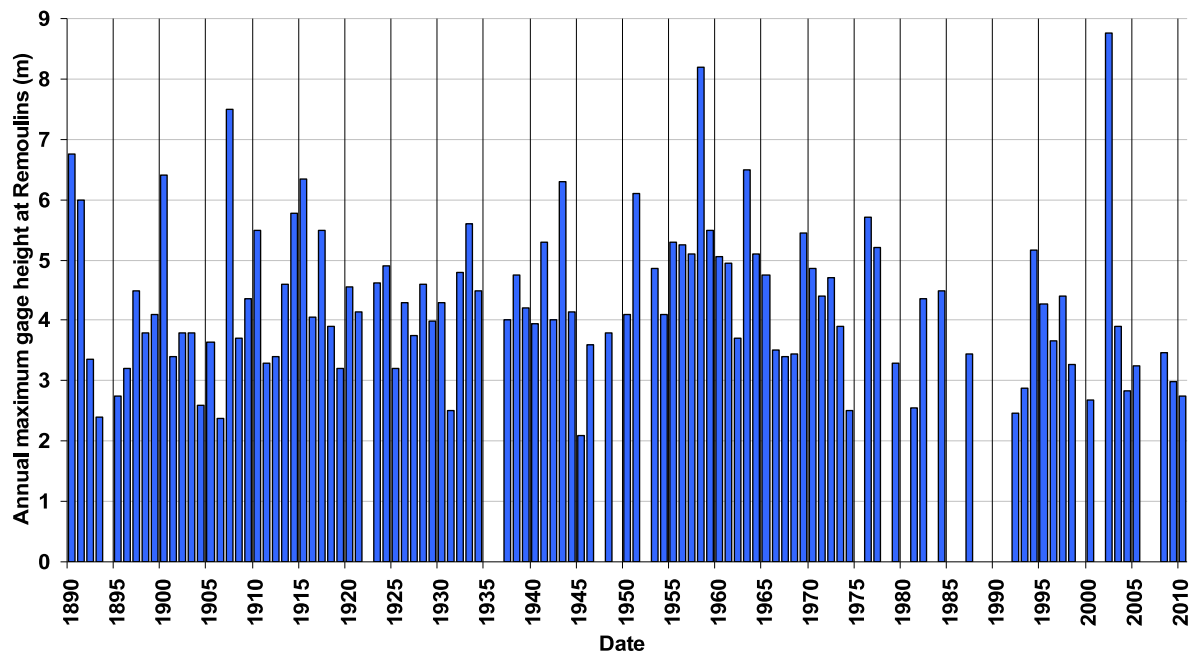
829

830 Table 1. Results from radiocarbon dating. All calibrated ages were calculated within 2σ .
831 Calibration was carried out using CALIB 6.1.0. The age model integrates the minimum and the
832 maximum value of the calibrated age.



833

834 Fig. 1: Topography, hydrography, and geological maps of the Gardon river watershed.



835
836
837

Fig. 2: Annual maximum gage height available at Remoullins between 1890 and 2010.

(A)



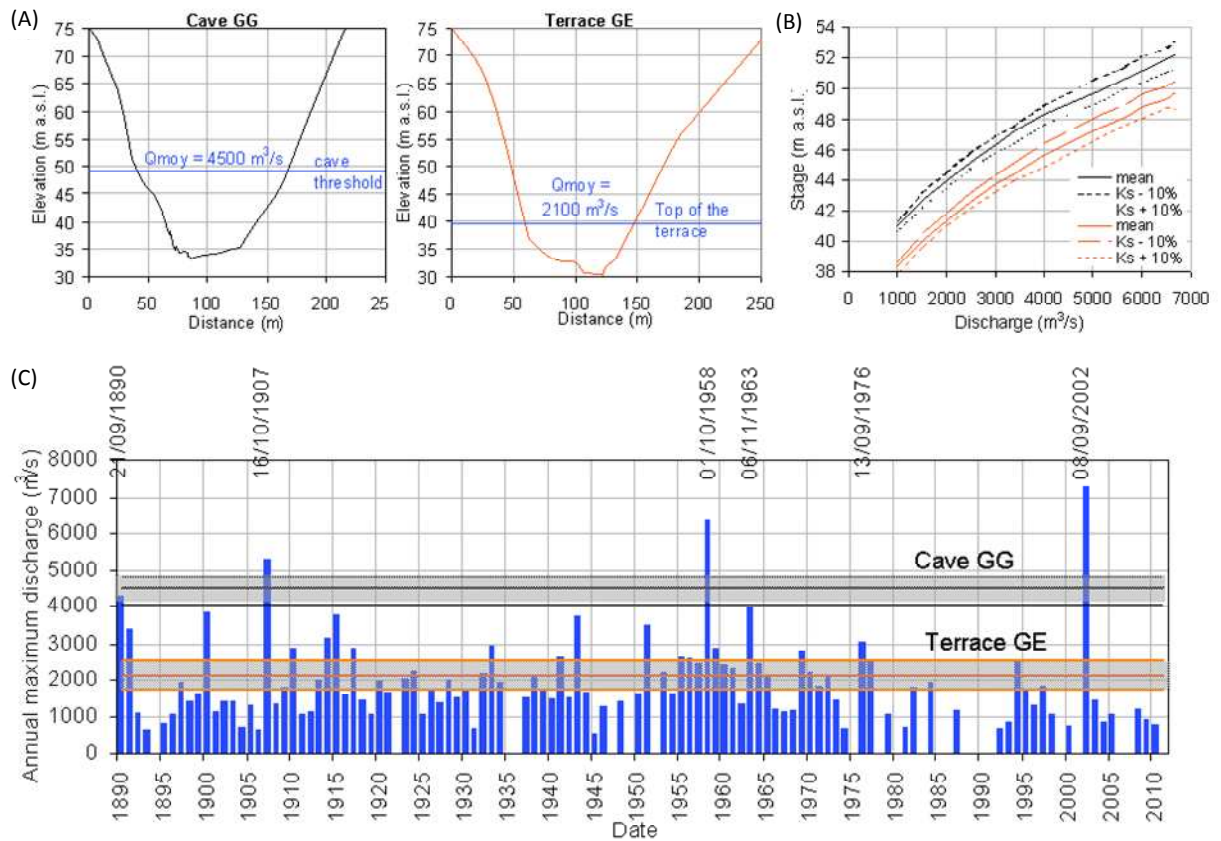
(B)



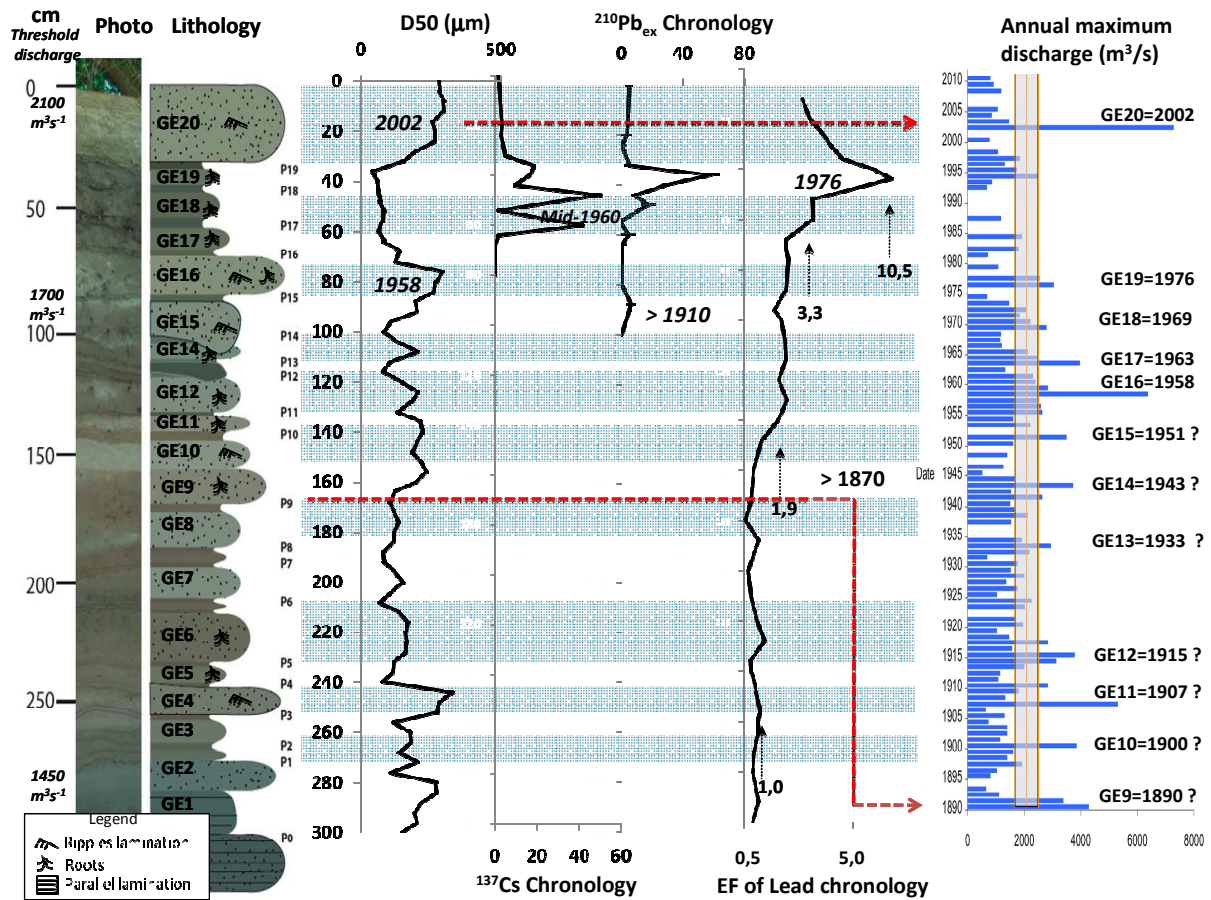
838

839 Fig. 3: (A) A map showing the study sites in the Gardon Gorges. (B) Terrace (GE) and cave

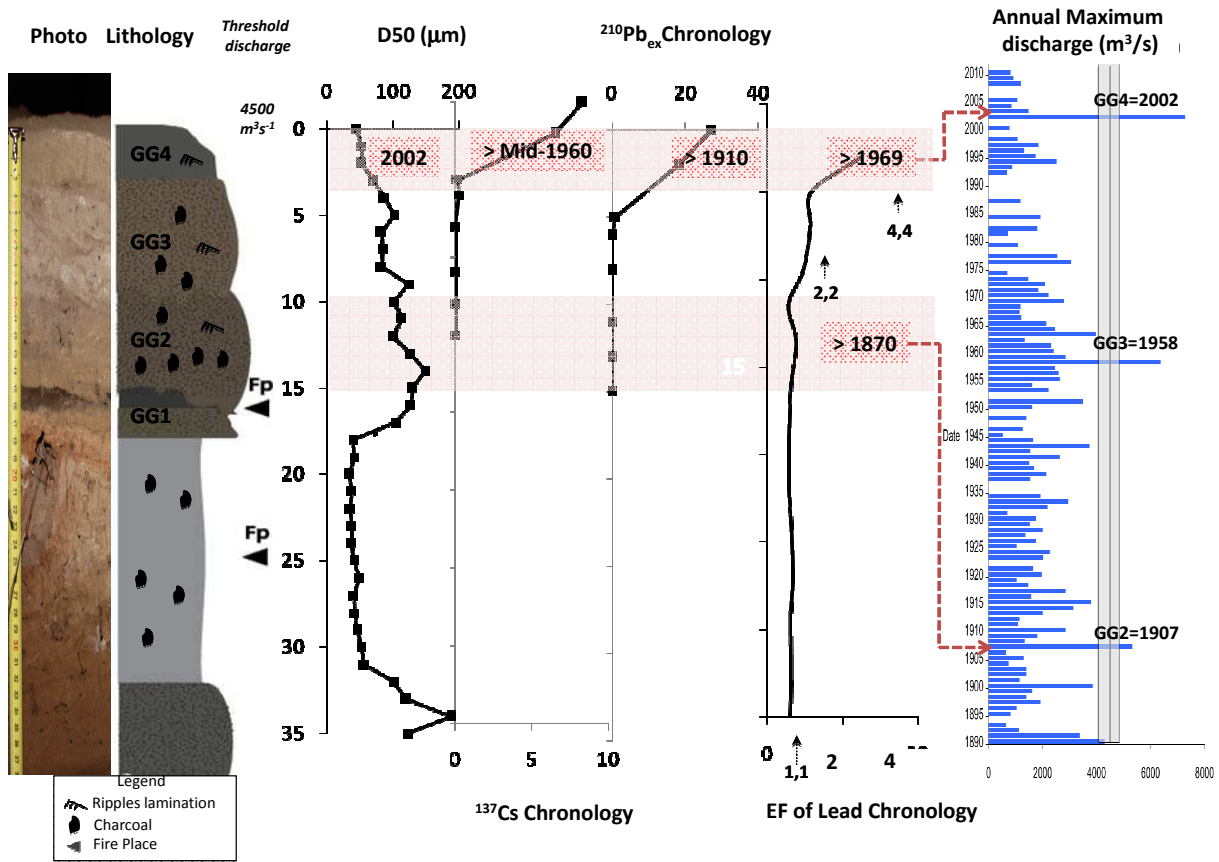
840 (GG), sites of slackwater flood sediment archives .



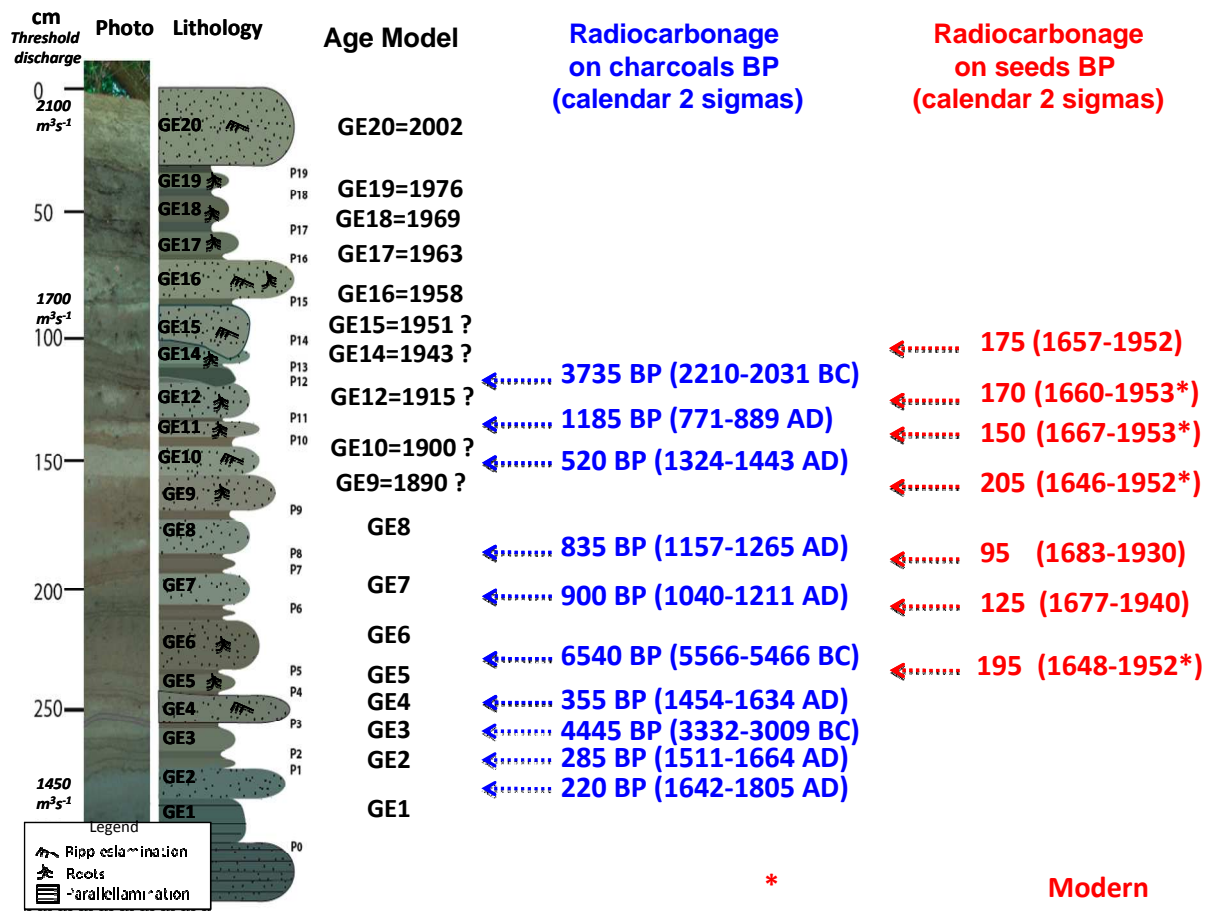
841 Fig. 4 (A) Cross sections of the paleosites used in the model; (B) Calculated stage-discharge
842 relationships and their envelope and (C) Historical flood series at Remoulins.



843 Fig. 5. The proposed chronology for the terrace GE slackwater flood deposits, d50, ¹³⁷Cs
 844 activities, ²¹⁰Pb_{ex} activities, EF of lead, the peak annual instantaneous discharges series at
 845 Remoulins. The envelope on the range of discharges at Remoulins that may have submerged the
 846 site resulting from the sensitivity analysis is shown. The individual slackwater flood units
 847 deposited by a particular event are annotated.



848 Fig. 6. The proposed chronology for the cave GG slackwater flood deposits, d50, ¹³⁷Cs activities,
 849 ²¹⁰Pb_{ex} activities, the peak annual instantaneous discharges series at Remoulins. The envelope on
 850 the range of discharges at Remoulins that may have submerged the site resulting from the
 851 sensitivity analysis is shown. The individual slackwater flood units deposited by a particular
 852 event are annotated.



853

854 Fig. 7. Stratigraphy and age model of site GE. Radiocarbon ages on wood charcoals (in blue) and
 855 seeds (in red) in BP and calendar ages (2σ)

856

857 Table 1. Results from radiocarbon dating. All calibrated ages were calculated within 2σ .
 858 Calibration was carried out using CALIB 6.1.0. The age model integrates the minimum and the
 859 maximum value of the calibrated age.

Sample	Type	Age	Calibrated age (agreement % Age model)	
GE113-116	charcoal	3735±35	2210-2031 BC (94%)	2210-2031 BC
GE 132-135	charcoal	1185±30	771-899 AD (92%)	771-899 AD
GE 148-152	charcoal	520±30	1324 1345 AD (10%) 1393-1443 AD (89%)	1324-1443 AD
GE 192-195	charcoal	835±30	1157-1265 AD (100%)	1157-1265 AD
GE 208-214	charcoal	900±30	1040-1110 AD (44%) 1115-1211 AD (55%)	1040-1211 AD
GE 238-243	charcoal	6540±40	5566-5466 BC (92%)	5566-5466 BC
GE 257-262	charcoal	355±35	1454-1529 AD (47%) 1540-1634 AD (53%)	1454-1634 AD
GE 267-270	charcoal	4445±35	3332-3213 BC (38%) 3132-3009 BC (51%)	3332-3009 BC
GE 275-280	charcoal	285±35	1511-1601 AD (61%) 1616-1664 AD (37%)	1511-1664 AD
GE 283-289	charcoal	220±30	1642-1683 AD (39%) 1735-1805 AD(48%)	1642-1805 AD
GE 103-107	seed	175±30	1657-1696 AD (19%) 1725-1814 AD (55%) 1917-1952* AD (20%)	1657-1952*AD
GE 122-127	seed	170±30	1660-1698 AD (18%) 1722-1817 AD (54%) 1916-1953* AD (20%)	1660-1953* AD
GE 138-142	seed	150±30	1667-1708 AD (17%) 1718-1783 AD (33%) 1796-1827 AD (12%) 1831-1889 AD (19%) 1910-1953* AD (19%)	1667-1953* AD
GE 157-161	seed	205±30	1646-1685 AD (29%) 1732-1808 AD (55%) 1928-1952* AD (16%)	1646-1952* AD
GE 188-193	seed	95±30	1683-1735 AD (28%) 1805-1930 AD (71%)	1683-1930 AD
GE 207-212	seed	125±30	1677-1766 AD (35%) 1800-1895 AD (47%) 1903-1940 AD (16%)	1677-1940 AD
GE 233-238	seed	195±30	1648-1691 AD (25%) 1729-1811 AD (57%) 1922-1952* AD (20%)	1648-1952*AD

860